Advances in Computational Design, *Vol. 2, No. 3 (2017) 211-223*
DOI: https://doi.org/10.12989/acd.2017.2.3.211

Seismic assessment of base-isolated nuclear power plants

Babak Farmanbordar[1], Azlan Bin Adnan[1], Mahmood Md. Tahir[2] and Iman Faridmehr[*2]

[1]*Engineering Seismology and Earthquake Engineering Research (e-SEER), Department of Structure and Materials, Universiti Teknologi Malaysia (UTM), 81300 Skudai, Johor Bahru, Malaysia*
[2]*UTM Construction Research Centre (CRC), Institute for Smart Infrastructures and Innovative Construction, Universiti, Teknologi Malaysia (UTM), Skudai, Johor Bahru, 81300, Malaysia*

(Received June 27, 2017, Revised July 3, 2017, Accepted July 4, 2017)

Abstract. This research presented a numerical and experimental study on the seismic performance of first-generation base-isolated and fixed-base nuclear power plants (NPP). Three types of the base isolation system were applied to rehabilitate the first-generation nuclear power plants: frictional pendulum (FP), high-damping rubber (HDR) and lead-rubber (LR) base isolation. Also, an Excel program was proposed for the design of the abovementioned base isolators in accordance with UBC 97 and the Japan Society of Base Isolation Regulation. The seismic assessment was performed using the pushover and nonlinear time history analysis methods in accordance with the FEMA 356 regulation. To validate the adequacy of the proposed design procedure, two small-scale NPPs were constructed at Universiti Teknologi Malaysia's structural laboratory and subjected to a pushover test for two different base conditions, fixed and HDR-isolated base. The results showed that base-isolated structures achieved adequate seismic performance compared with the fixed-base one, and all three isolators led to a significant reduction in the containment's tension, overturning moment and base shear.

Keywords: dynamic relaxation method; concentrated damping; form-finding; membrane structures

1. Introduction

The seismic performance of nuclear power plants (NPP) has always been difficult to predict because of the immediate occupancy performance level of this type of structure. In recent decades, NPPs have been subjected to severe natural disasters (i.e., earthquake, tornado, tsunami) and terrorist attacks. One of the most important disasters in recent years occurred in Fukushima Daiichi Nuclear Power Plant on March 11, 2011; see Fig. 1. After the Fukushima Daiichi nuclear disaster, the sufficiency of the seismic performance of first-generation nuclear power plants (FGNPP) was questioned. Accordingly, majority of the design guidelines provided a new design procedure or strategy to address this extreme loading requirement. One of the most effective methods of seismic rehabilitation of NPPs is using seismic base isolation (SBI). These energy dissipation devices consume seismic energy and lead to a safer situation.

∗Corresponding author, E-mail: s.k.k-co@live.com

http://www.techno-press.org/?journal=acd&subpage=7 ISSN: 2283-8477 (Print), 2466-0523 (Online)

Fig. 1 Fukushima Daiichi disaster during the earthquake in the Futaba District on March 11, 2011

A good number of published studies describe the application of seismic base isolation to nuclear power plants. The first serious discussions and analyses of SBI occurred in the 1980s, during which time Skinner *et al.* (Skinner *et al.* 1976) showed the growth of technology, paving the way to the investigation of the application of SBI to NPPs, which peaked in the mid-1980s, after the creation of French isolated NPP designs in Cruas, France, and Koeberg, South Africa, whose safe shutdown earthquake (SSE) acceleration limits were 0.2 g and 0.3 g, respectively. In another study, comparative dynamic analyses were performed on fixed-base and isolated nuclear plants (Tajirian *et al.* 1990). The obtained response spectra indicated major horizontal decreases at frequencies over 1.0 Hz and vertical decreases at frequencies over 4.0 Hz, covering the usual frequency ranges of the standard NPP equipment. Huang *et al.* (Huang *et al.* 2006, Huang, Whittaker *et al.* 2007, Huang *et al.* 2013, Whittaker *et al.* 2011) presented a comprehensive review of SBI systems' response when applied to NPPs using SAP2000. These SBI systems consist of either friction pendulum (FP), low-damping rubber (LDR), lead-rubber (LR) or high-damping rubber (HDR) bearings. Horizontal seismic motions were exerted on the fixed-base and isolated model, representing west and east coast sites at DBE and SSE levels so that the SBI effect could be monitored on the secondary systems in NPPs. In the case of NPPs that used SBI of all types, the obtained results demonstrated a significant decrease in the seismic demands on the secondary systems. More recent studies (Buckle and Mayes 1990, Cheraghi and Izadifarda 2013, Cho *et al.* 2015, Dhawade 2014, Huang 2008, Huang *et al.* 2007, Huang *et al.* 2010, Releasable 1978, Sayed *et al.* 2015, Tamayo and Awruch 2016) have confirmed that in base-isolated nuclear structures, the accelerations and deformations in structures, systems and components (SSCs) are relatively small. SSCs are expected to remain elastic for both design basis earthquake (DBE) shaking and beyond DBE. As such, the unacceptable performance of an isolated nuclear structure will most likely involve either the failure of isolation bearings or the impact of the isolated superstructure and the surrounding building or geotechnical structures.

Literature reviews have indicated that far too little attention has been paid to experimental research on the effects of seismic load on an isolated NPP. Besides, there has been little discussion on the performance of an isolated NPP under seismic loads with respect to the new criteria and

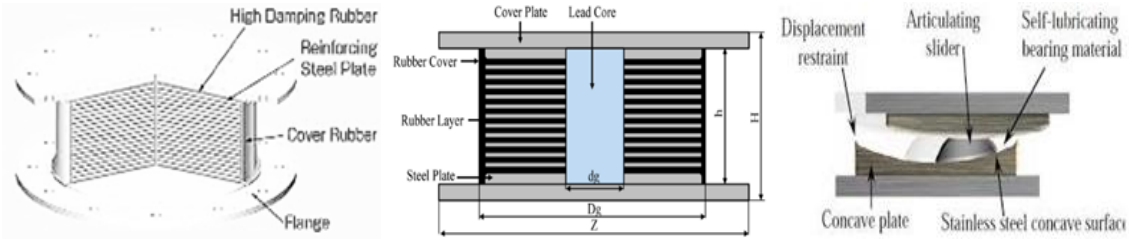

(a) (b) (c)

Fig. 2 Schematic of high-damping rubber (HDR) (a), lead-rubber (LR) (b) and friction pendulum (FP) (c) isolation system

conditions of current norms and practices. This research critically investigates the seismic performance of a fixed-base and an isolated NPP retrofitted with three types of base isolation. Moreover, two small-scale fixed and isolated-base NPPs subjected to a pushover test were experimentally investigated.

2. Seismic base isolation

As a structural technology, SBI can reduce superstructural accelerations and at the same time limit interstory drifts. Different types of SBI devices have been designed, all of which are laterally flexible relative to the superstructure. Through the placement of isolators between the superstructure and the foundation, a laterally flexible layer that decouples the structure from the ground will be provided. As demonstrated in Eq. (1), for a single-degree-of-freedom (SDOF) system wherein mass, *m*, is held constant, the horizontal dynamic vibration period, *T*, is inversely proportional to the square root of lateral stiffness, *k*. Therefore, even for multiple-degree-of-freedom (MDOF) systems, a considerable decline of stiffness can lead to an important lengthening of the fundamental horizontal period.

$$T = \frac{2\pi}{\omega} = 2\pi\sqrt{\frac{m}{k}} \tag{1}$$

In high-damping rubber (HDR) isolators, alternating bonded elastomer and steel laminates provide lateral flexibility while remaining stable and stiff in a vertical state as shown in Fig. 2(a). The thickness of the rubber layers controls the horizontal and vertical stiffness and displacement capacity. To limit the thickness of the individual rubber layers, steel plates are used, thereby reducing bulging and ensuring that the isolator deforms in shear as opposed to bending. This type of isolator uses an equivalent linear viscous damping between 10% and 20% (Naeim and Kelly 1999), and it can produce an advantageous nonlinear response. Lead-rubber (LR) isolators or lead-plug bearings (Robinson 1982) make use of low-damping natural rubber and dissipate energy by obtaining one or more lead plugs that are vertically embedded in the bearing, which provides a restoring action; see Fig. 2(b). In general, the LR bearings are created for shear strains of up to 200% and damping ratios of 35% (Jeon *et al.* 2015). As indicated in laboratory tests, elastomeric bearings can reach shear strains exceeding 400% before failure (Konstantinidis *et al.* 2008). In frictional isolators, a low-friction interface is found between the superstructure and the foundation,

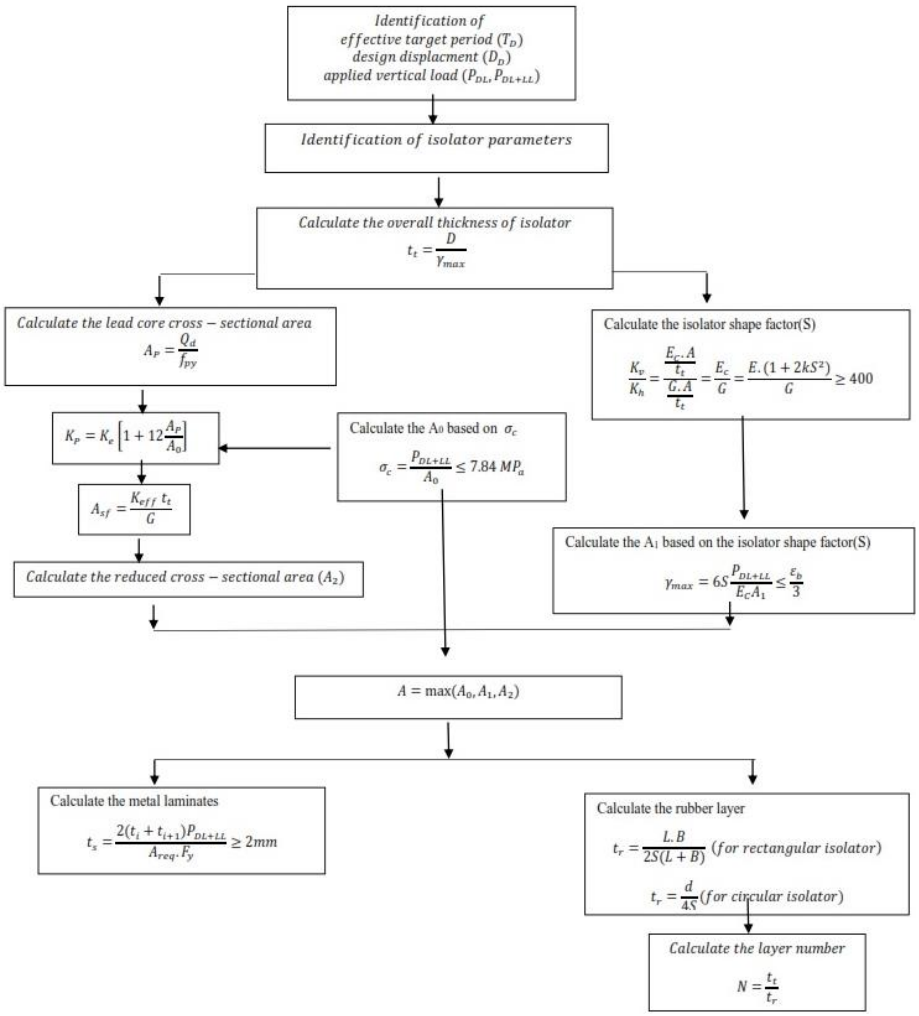

Fig. 3 Design flowchart for an elastomeric and LR base isolation system

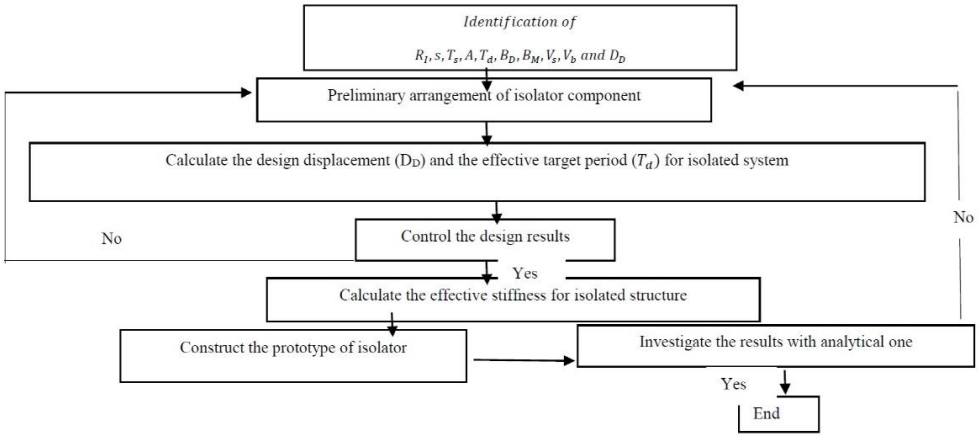

Fig. 4 Design flowchart for frictional bearings base isolation system

Table 1 Dimensions of the three base isolations used in the time history analysis

Component of Isolation Type	Value
High-damping rubber bearing (HDR)	
Height	330 (mm)
Diameter	1450 (mm)
Number of rubber layers	8
Thickness of rubber layers	40 (mm)
Effective stiffness	2428 (kN/m)
Effective damping	20%
Lead-rubber bearing (LR)	
Height	330 (mm)
Diameter	1450 (mm)
Number of rubber layers	8
Thickness of rubber layers	40 (mm)
Diameter of lead core	21 (mm)
Effective stiffness	2426 (kN/m)
Secondary stiffness	1664 (kN/m)
Effective damping	20%
Friction pendulum bearing (FP)	
Height	150 (mm)
Diameter	1620 (mm)
Curve radius	1550 (mm)
Effective stiffness	2850 (kN/m)
Effective damping	10%

confining the transmittable force; see Fig. 2(c). Contrary to elastomeric isolators, which are composed of chemical bonds between different elements, most sliding bearings are dependent on gravity for maintaining contact between surfaces. These types of bearings are able to transfer tension; nonetheless, they are less commonly used.

The design of seismic base isolation systems begins with a consideration of vertical loads and continues with the determination of a target horizontal displacement and ends with the checking of the stability and horizontal displacement of the isolation system. An Excel program has been prepared by authors for designing base isolators based on the Uniform Building Code (UBC)(ICC) 1997) and the Japan Society of Base Isolation (Pan *et al.* 2005). Figs. 3 and 4 show the steps of this Excel program.

3. Experimental and numerical simulation

3.1 Loading protocol

The evaluation of the base-isolated NPP was considered through pushover and time history analyses. For the pushover analysis, the horizontal loading gradually increases at the top of the specimen and continues until totally collapsing based on the FEMA 356 (FEMA 356-Prestandard and Commentary for the Seismic Rehabilitation of Buildings 2000) regulation. The target displacements for isolated and nonisolated NPPs in compliance with the coefficient method are 80 cm and 20 cm, respectively. In this analysis, a small-scale specimen with a fixed base and an HDR

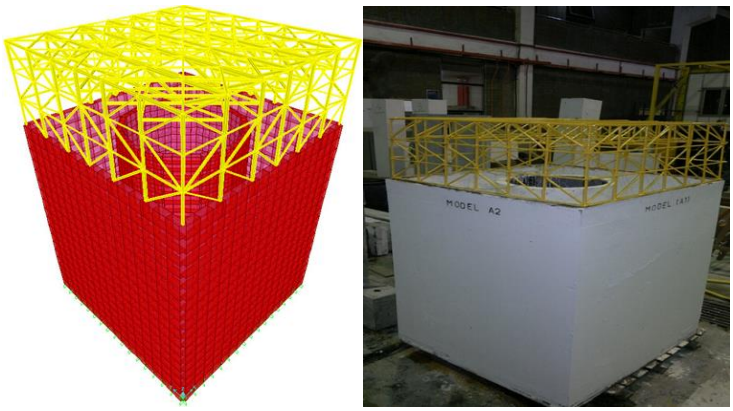

Fig. 5 Numerical and experimental model of the Fukushima NPP

isolator was considered in which the analysis consisted of the application of gravity loads and a representative lateral load pattern. On the other hand, for the time history analysis, the structural response, such as fundamental periods of structures, tension of NPP containment, overturning moment and base shears, was obtained under the Imperial Valley earthquake for fixed-base and LR-, FP- and HDR-isolated structures.

3.2 Case studies under investigation

For the time history analysis, a case study was designed based on the Fukushima NPP, which was a boiling water reactor (BWR). The specimen was 43.0 m tall with a 40.0 m square footprint of side length. The exterior containments were 1.2 m thick, and the interior walls were 1.4 m thick. The isolation slab was 2.0 m thick. Three base isolation systems (LR, FP, HDR) were considered to evaluate the seismic performance of the base-isolated NPPs in comparison with a fixed-based one. Details of the abovementioned base isolation designed in accordance with the proposed flowchart are illustrated in Table 1.

Meanwhile, for the pushover analysis, a specimen with 1/36th of the real scale was constructed at the structural laboratory of Universiti Teknologi Malaysia. The pushover analysis consisted of the application of gravity loads and a representative lateral triangular load pattern (TLP). The lateral loads were applied monotonically step-by-step using a hydraulic jack in the X direction based on FEMA 356 (FEMA 356-Prestandard and Commentary for the Seismic Rehabilitation of Buildings 2000) recommendations. The isolator used in this test had an overall thickness of 7 cm and a steel laminate thickness of 2 mm. In this particular analysis, a comparison was made between a fixed-base and an HDR-base-isolated specimen only. Fig. 5 shows the numerical and experimental model used in this study.

4. Results and discussion

This section presents the numerical and experimental results for the base-isolated and fixed-base NPPs subjected to nonlinear time history (dynamic) and pushover loads. The results consisted of nonlinear time history (NLTH) and pushover analyses for fixed-base NPPs and HDR-, LR- and

Table 2 Four first periods of fixed- and isolated-base specimens

Mode	FB Period sec	FPBI Period sec	LRBI Period sec	HDRBI Period sec
1	0.249	3.155	3.438	3.436
2	0.193	2.11	2.299	2.297
3	0.193	2.11	2.299	2.297
4	0.171	0.672	0.721	0.721

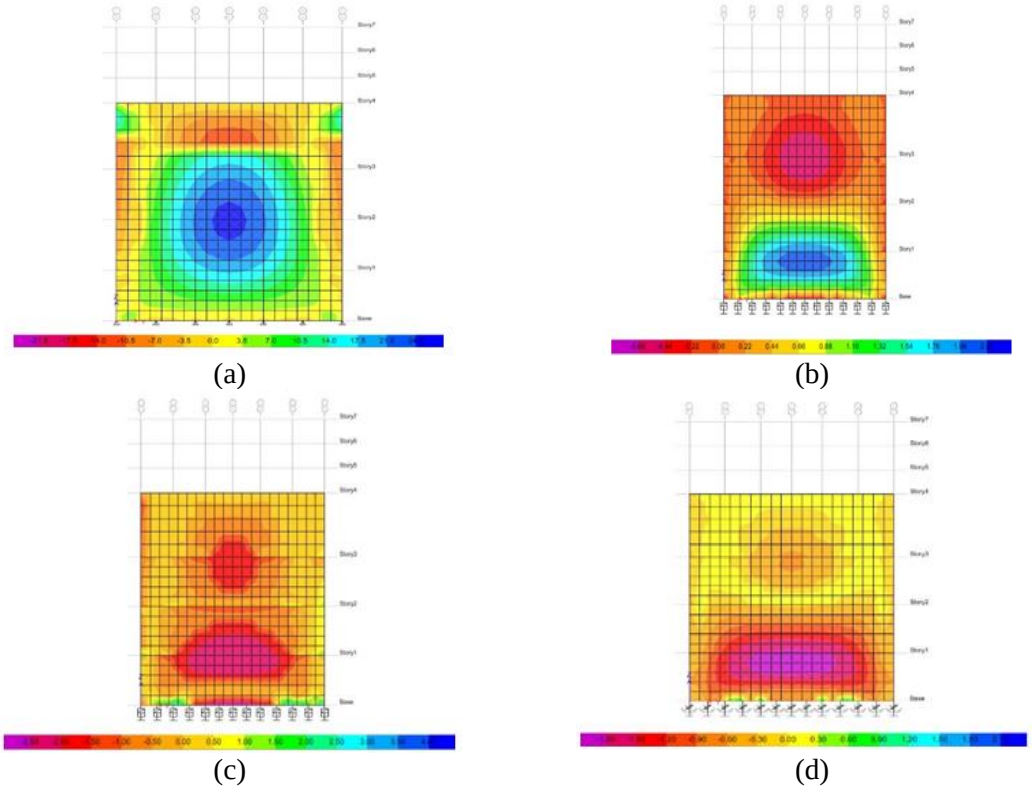

(a) (b) (c) (d)

Fig. 6 Stress distribution at the fixed-base- (a), HDR-base- (b), LR-base- (c) and FP-base- (d) isolated NPP subjected to time history analysis

FP-base-isolated NPP. The fundamental parameters considered in this evaluation were base shear versus horizontal displacement for the pushover tests and stress distribution at the wall for the NLTH test. A brief summary of the results for the damaged state at the end of the NLTH and pushover tests is also included in this section.

4.1 Fundamental periods of structures

During a structural dynamic analysis, a fundamental period is taken into consideration to describe the stiffness of the superstructure. This period can also be used properly in preliminary analyses. Table 2 provides a comparison of four first periods between fixed- and isolated-base NPPs. The results show a significant increase of period using base isolation.

Table 3 The maximum tension of containment

Base Type	Tension of Containment (N/mm^2)
FB	17.69
FP	1.58
LR	1.93
HDR	2.11

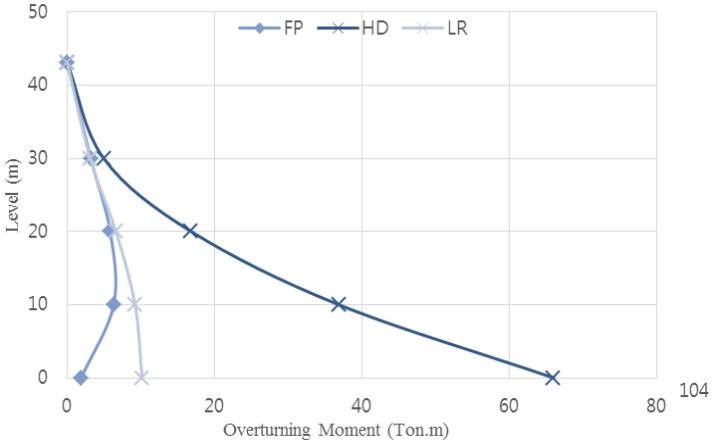

Fig. 7 Overturning moment of containment

4.2 Tension of NPP containment

Fig. 6 shows the tension results for the NPP containment with different base types. The cracking tension and yield forces of the bilinear hinges are fundamental parameters in the seismic evaluation of NPP containment. The cracking tension for concrete was estimated using f_r=0.62 $f'_c{}^{0.5}$, as mentioned in ACI 349-01(349 2001), where f'_c is the compressive strength. The value of 35 N/mm^2 was used in this study based on compressive strength tests of concrete cube. The yield forces of the bilinear hinges were estimated using 0.5 $f_c'A_S$, in accordance with ACI 349-01(349 2001), where A_s is the shear area reinforcement.

Table 3 shows the maximum tension of containment with the fixed and the isolated base subjected to nonlinear time history analysis. Based on Table 3, the FP base isolator clearly has maximum effectiveness on the tension of containment with a reduction of 91% compared with the fixed-base specimen. Subsequently, the LR and the HDR base isolation system provided less stress tension on containment with a reduction of 90% and 88%, respectively, compared with the fixed-base specimen.

4.3 Overturning moment consideration

Fig. 7 shows the overturning moment of containment equipped with the FP, HDR and LR base isolation systems subjected to time history analysis. Fig. 7 indicates that, generally, the overturning moment is decreased by increasing the containment level. However, the overturning moment of FP-base-isolated NPP involves an erratic behaviour. Besides, Fig. 7 shows that the

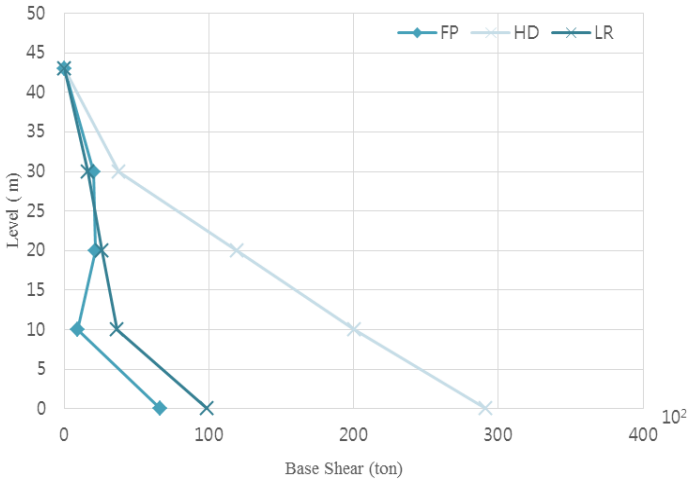

Fig. 8 Base shear of containment

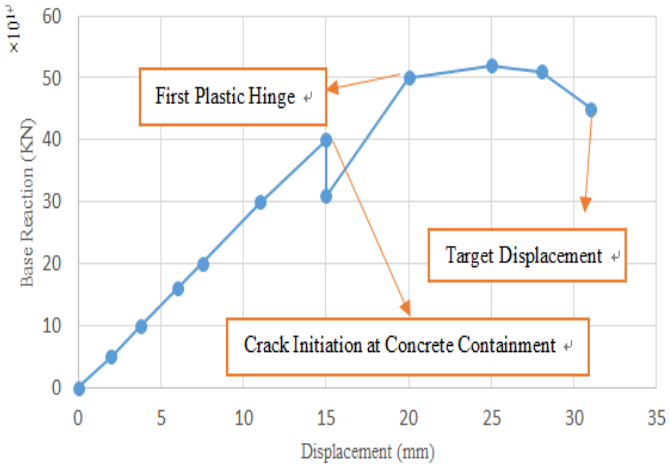

Fig. 9 Pushover curve of the FB nuclear power plant

HDR base isolator provides conservative results compared with the LR and FP base isolators as the overturning moment is around six times higher. All in all, the overturning moment of containment had severe reduction by using the base isolation system compared with the fixed-base one (200×10^4 ton.m).

4.4 Base shears

Base shear is a significant parameter for the seismic assessment of NPP. Generally, using base isolation leads to a significant decrease in base shear. For example, in this study the base shear was reduced from 8000×10^2 ton for the fixed-base isolator to 300×10^2 ton for the HDR-base isolator. Fig. 8 shows the shear versus the containment level for the LR-, FP- and HDR-base isolators subjected to time history analysis. This figure indicates that the base shear had reduction by going to the upper level; however, the LR- and FP-base isolators showed an irregular behaviour. Also,

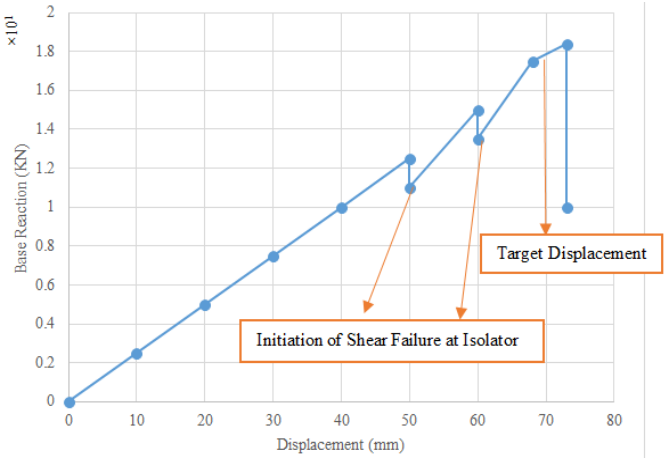

Fig. 10 Pushover curve of the HDR nuclear power plant

Fig. 11 Damaged state of the FB and HDR specimens at the final step of the pushover test

the HDR isolator clearly led to a higher base shear compared with the FP- and LR-base isolators.

4.5 Pushover analysis of small-scale NPP with the FB- and the HDR-base isolator

Figs. 9 and 10 show the pushover curve for the FB and HDR nuclear power plants. Based on Fig. 9, the FB nuclear power plant experienced a significant base shear compared with the HDR nuclear power plant; however, the horizontal displacement at the final stage in this specimen was 0.4 of the HDR specimen. Also, the FB specimen did not address the FEMA 356 requirements as it had plastic hinges beyond immediate occupancy level earlier reaching the target displacement. Nevertheless, this specimen showed a much more nonlinear behaviour than the HDR specimen. Fig. 10 shows that the specimen resists up to the target displacement without plastic hinge formation in the main structure component. It was noticed that a minor failure only occurred in the HDR isolator at the final stage because of extraordinary shear force.

Considering the nominal yield strain of 1800 $\mu\varepsilon$ (microstrain) for the reinforcement bar, higher strain readings in the range of 5000-5800 $\mu\varepsilon$ (i.e., almost three times above the yield level) were

obtained at FB containment, indicating that this component was in the plastic range during the testing process. On the other hand, the HDR nuclear power plants delimited the strains at the base isolator portions, and therefore, the main structure maintained its elastic behaviour throughout the loading scenario. Fig. 11 indicates the damaged state of the FB and HDR nuclear power plants after the final step of the pushover test.

5. Conclusions

This study evaluated the seismic response of fixed-base and base-isolated nuclear power plants in accordance with the Uniform Building Code (UBC) and the Japan Society of Base Isolation through a series of experimental and numerical investigations. Pushover and NLTH analyses in accordance with FEMA 356 were considered for seismic assessment where base shear and cracking tension and yield forces of the containment were fundamental parameters in the seismic evaluation of NPP. Based on the results of the experimental and numerical analyses, the following conclusions have been drawn:

i. The NPP containment remained in an elastic region for the base isolation, where shear failure only appeared in the base isolation, and no crack was reported for the concrete containment during the test.

ii. A comparison between LR-, FP- and HDR-isolated structures revealed that all these three isolators led to a significant reduction in the containment's tension, overturning moment and base shear. Also, the HDR isolation system provided unconservative results compared with the LR and the FP isolation system.

iii. The experimental test showed that the base isolation system provides adequate response to maintain an immediate occupancy level before reaching the target displacement.

Acknowledgements

The authors wish to thank the esteemed technical staff of the Laboratory of Structures and Materials, Universiti Teknologi Malaysia (UTM), for their cooperation and support for this study. They would also like to express their appreciation for the financial support provided by Universiti Teknologi Malaysia (UTM) for the conduct of the experimental work.

References

349 A.C. (2001), *Code Requirements for Nuclear Safety Related Concrete Structures (ACI 349-01)*, In A.C. Institute (Ed.).

(ICC), I.C.C. (1997), *Uniform Building Code (UBC)*, International Council of Building Officials, U.S.A.

Buckle, I.G. and Mayes, R.L. (1990), "Seismic isolation: History, application, and performance-a world view", *Earthq. Spectr.*, **6**(2), 161-201.

Cheraghi, R.E. and Izadifarda, R.A. (2013), "Demand response modification factor for the investigation of inelastic response of base isolated structures", *Earthq. Struct.*, **5**(1), 23-48.

Cho, S.G., Yun, S.M., Kim, D. and Hoo, K.J. (2015), "Analyses of vertical seismic responses of seismically isolated nuclear power plant structures supported by lead rubber bearings", *J. Earthq. Eng. Soc. Kor.*,

19(3), 133-143.
Dhawade, S. (2014). "Comparative study for seismic performance of base isolated & fixed base RC frame structure", *J. Civil Eng. Res.*, **5**, 183-190.
FEMA 356-Prestandard and Commentary for the Seismic Rehabilitation of Buildings (2000), American Society of Civil Engineers, Washington, U.S.A.
Huang, Y.N. (2008), *Performance Assessment of Conventional and Base-Isolated Nuclear Power Plants for Earthquake and Blast Loadings*, ProQuest.
Huang, Y.N., Whittaker, A.S. and Constantinou, M.C. (2006), *Seismic Demands on Secondary Systems in Conventional and Isolated Nuclear Power Plants*.
Huang, Y.N., Whittaker, A.S., Constantinou, M.C. and Malushte, S. (2007), "Seismic demands on secondary systems in base-isolated nuclear power plants", *Earthq. Eng. Struct. Dyn.*, **36**(12), 1741-1761.
Huang, Y.N., Whittaker, A.S., Kennedy, R.P. and Mayes, R.L. (2013), "Response of base-isolated nuclear structures for design and beyond-design basis earthquake shaking", *Earthq. Eng. Struct. Dyn.*, **42**(3), 339-356.
Huang, Y.N., Whittaker, A.S. and Luco, N. (2010), "Seismic performance assessment of base-isolated safety-related nuclear structures", *Earthq. Eng. Struct. Dyn.*, **39**(13), 1421-1442.
Jeon, B.G., Choi, H.S., Hahm, D.G. and Kim, N.S. (2015), "Seismic fragility analysis of base isolated NPP piping systems", *J. Earthq. Eng. Soc. Kor.*, **19**(1), 29-36.
Konstantinidis, D., Kelly, J.M. and Makris, N. (2008), *Experimental Investigation on the Seismic Response of Bridge Bearings*, Earthquake Engineering Research Center, University of California, U.S.A.
Naeim, F. and Kelly, J.M. (1999), *Design of Seismic Isolated Structures: From Theory to Practice*, John Wiley & Sons.
Pan, P., Zamfirescu, D., Nakashima, M., Nakayasu, N. and Kashiwa, H. (2005), "Base-isolation design practice in Japan: Introduction to the post-Kobe approach", *J. Earthq. Eng.*, **9**(1), 147-171.
Releasable, P. (1978), "Development of criteria for seismic review of selected nuclear power plants", *Urban.*, **51**, 61801.
Robinson, W.H. (1982), "Lead-rubber hysteretic bearings suitable for protecting structures during earthquakes", *Earthq. Eng. Struct. Dyn.*, **10**(4), 593-604.
Sayed, M.A., Go, S., Cho, S.G. and Kim, D. (2015), "Seismic responses of base-isolated nuclear power plant structures considering spatially varying ground motions", *Struct. Eng. Mech.*, **54**(1), 169-188.
Skinner, R., Tyler, R. and Hodder, S. (1976)., "Isolation of nuclear power plants from earthquake attack", *Bullet. New Zealand Nat. Soc. Earthq. Eng.*, **9**(4), 199-204.
Tajirian, F.F., Kelly, J.M. and Aiken, I.D. (1990), "Seismic isolation for advanced nuclear power stations", *Earthq. Spectr.*, **6**(2), 371-401.
Tamayo, J.L.P. and Awruch, A.M. (2016), "Numerical simulation of reinforced concrete nuclear containment under extreme loads", *Struct. Eng. Mech.*, **58**(5), 799-823.
Whittaker, A., Huang, Y., Mayes, R. and Kennedy, R. (2011), *Seismic Isolation of Safety-Related Nuclear Structures*, ASCE.

TK

Nomenclature

D_D	Maximum design displacement of a response spectrum
K_{eff}	Minimum effective stiffness of the isolation system at the design displacement in the horizontal direction under consideration

T_D	Target displacement
B or L	Length of isolator
t_t	Overall thickness of isolator
t_r	Thickness of rubber layers
N	Number of rubber layers
t_s	Thickness of steel laminates
γ_{max}	Maximum shear relative displacement capacity of rubber (1 ≈ 1.5)
G	Shear modulus of rubber (0.69 ≈ 0.86 MPa)
σ_c	Allowable stress of isolator (6.9 ≈ 7.84 MPa)
E	Rubber modulus of elasticity (1.5 ≈ 5 MPa)
K_v	Vertical stiffness of isolator
K_h	Horizontal stiffness of isolator
E_c	Compression modulus of rubber and metal laminates combination
K	Modification factor (1≈1.5)
S	Configuration factor
A_0, A_1, A_2	Required isolator area
A_{sf}	Required isolator area to prevent shear rupture
t_i, t_{i+1}	Thickness of rubber layer top and bottom of metal laminate
f_y	Yield stress of metal laminates
Q_d	Allowable stress of isolator with lead core
f_{py}	Yield stress of lead core
A_p	Cross-sectional area of lead core
K_p	Bilinear stiffness of isolator with lead core
ε_b	Maximum tension relative displacement capacity of rubber
R_{I}	Behaviour factor of isolated structure
$\mathrm{T_d}$, T_s, S	Design response spectrum parameters
B_D, B_M	Damping coefficients
V_s	Base shear of structural component above isolation level
V_b	Base shear of structural component below isolation level